Volume 4
Number 7
July 2024
Pages 701–832

Environmental Science Atmospheres

rsc.li/esatmospheres

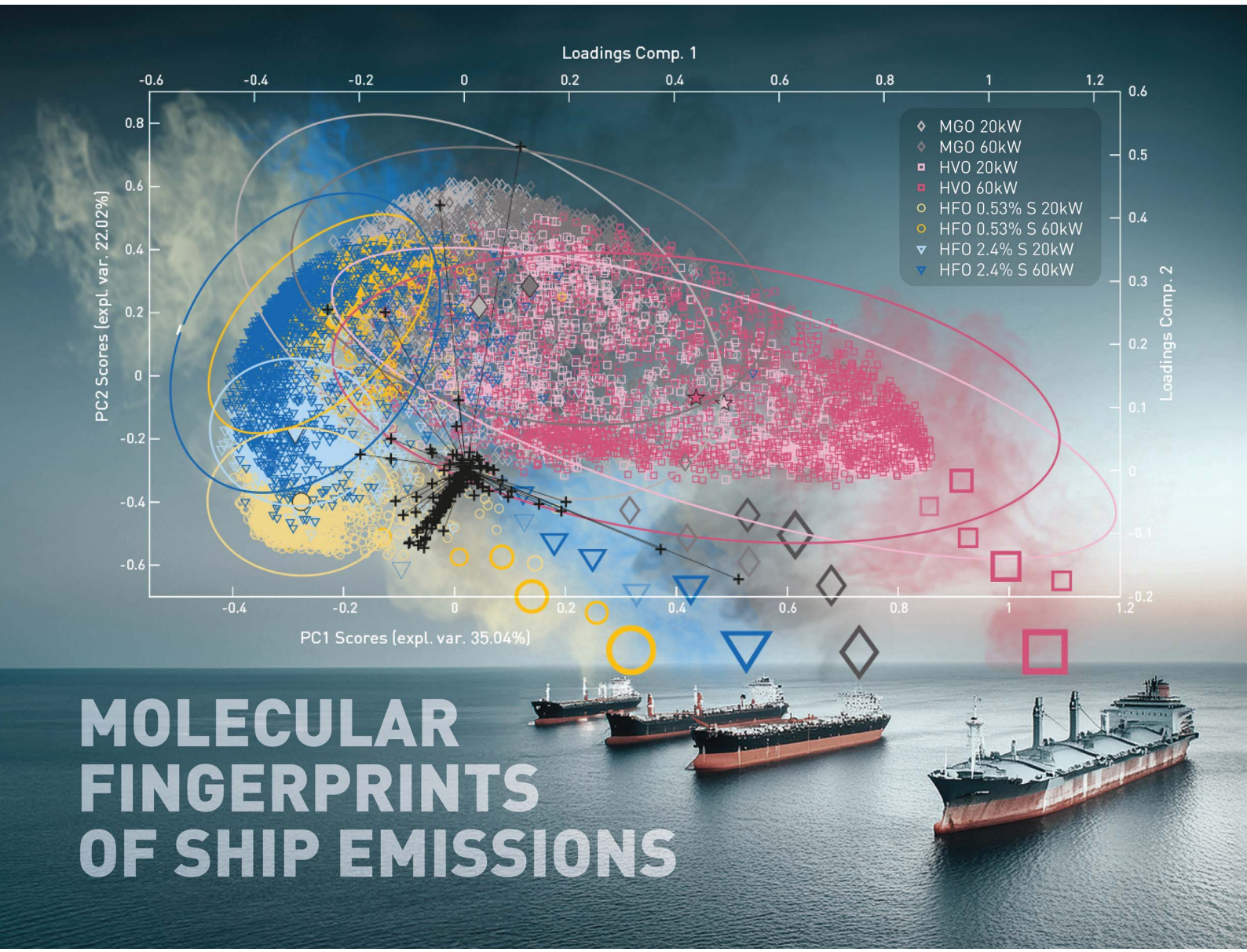

MOLECULAR FINGERPRINTS OF SHIP EMISSIONS

ISSN 2634-3606

ROYAL SOCIETY OF CHEMISTRY

PAPER
Johannes Passig *et al.*
Polycyclic aromatic hydrocarbons as fuel-dependent markers in ship engine emissions using single-particle mass spectrometry

Environmental Science: Atmospheres

ROYAL SOCIETY OF CHEMISTRY

PAPER

View Article Online
View Journal | View Issue

Open Access Article. Published on 20 May 2024. Downloaded on 11/15/2025 2:34:17 AM.
This article is licensed under a Creative Commons Attribution 3.0 Unported Licence.

Check for updates

Cite this: *Environ. Sci.: Atmos.*, 2024, **4**, 708

Polycyclic aromatic hydrocarbons as fuel-dependent markers in ship engine emissions using single-particle mass spectrometry†

Lukas Anders,[ab] Julian Schade,[abc] Ellen Iva Rosewig,[ab] Marco Schmidt,[ab] Robert Irsig,[d] Seongho Jeong,[abc] Uwe Käfer,‡[a] Thomas Gröger,[a] Jan Bendl,[ac] Mohammad Reza Saraji-Bozorgzad,[acd] Thomas Adam,[ac] Uwe Etzien,[e] Hendryk Czech,[a] Bert Buchholz,[e] Thorsten Streibel,[ab] Johannes Passig *[ab] and Ralf Zimmermann[ab]

Received 24th March 2024
Accepted 18th May 2024

DOI: 10.1039/d4ea00035h

rsc.li/esatmospheres

We investigated the fuel-dependent single-particle mass spectrometric signatures of polycyclic aromatic hydrocarbons (PAHs) from the emissions of a research ship engine operating on marine gas oil (MGO), hydrotreated vegetable oil (HVO) and two heavy fuel oils (HFO), one with compliant and one with non-compliant fuel sulfur content. The PAH patterns are only slightly affected by the engine load and particle size, and contain sufficient dissimilarity to discriminate between the marine fuels used in our laboratory study. Hydrotreated vegetable oil (HVO) produced only weak PAH signals, supporting that fuel residues, rather than combustion conditions, determine the PAH emissions. The imprint of the fuel in the resulting PAH signatures, combined with novel single-particle characterization capabilities for inorganic and organic components, opens up new opportunities for source apportionment and air pollution monitoring. The approach is independent of metals, the traditional markers of ship emissions, which are becoming less important as new emission control policies are implemented and fuels become more diverse.

Environmental significance

Ship emissions are a major source of air pollution, causing serious impacts on human health, environment and climate. Various sulfur emission regulations have come into force in recent years, leading to a diversification of marine fuels. As a result, there is a need for alternatives to the traditional markers of ship emissions, taking into account the new fuel types. Here we show how the characteristic signatures of polyaromatic hydrocarbons can be used to identify the fuel for the purposes of monitoring and surveillance.

Introduction

Global shipping has a significant impact on human health, ecosystem quality and climate change through the release of anthropogenic emissions such as carbon dioxide (CO_2), sulfur oxides (SO_X), nitrogen oxides (NO_X) and particulate matter (PM) into the atmosphere.[1–6] Maritime transport facilitates over 90% of global trade volume,[7] and trends indicate that demand for shipping will increase by up to 50% by 2030 compared to 2016 levels.[8] To reduce the environmental and health burden, sulfur emission control areas (SECAs) have been established in many coastal regions (*e.g.* North America, North Sea, Baltic Sea, United States Caribbean Sea[9]), limiting the fuel sulfur content (FSC). The current EU sulfur directives require ships to use fuels with a maximum FSC of 0.1% m m^{-1} inside SECAs since 2015.[9] A global sulfur cap of 0.5% m m^{-1} outside SECA zones was put in place in 2020.[10] As a result, the range of fuels available has diversified, including bunker fuels ("Heavy Fuel Oils", HFOs) with varying sulfur contents. The majority of ships operating in SECAs have transitioned to use distillate fuels such as marine gas oil (MGO).[11] This has resulted in a significant reduction in particulate matter (PM) emissions.[12,13] However, it is important to recognize that the use of low sulfur containing fuels without filter technology may still have a substantial impact on human health.[14]

[a]Joint Mass Spectrometry Centre, Analytical Chemistry, University of Rostock, Helmholtz Centre Munich, Comprehensive Molecular Analytics, 85764 Neuherberg, 18059 Rostock, Germany. E-mail: lukas.anders2@uni-rostock.de; johannes.passig@uni-rostock.de

[b]Department Life, Light & Matter, University of Rostock, 18059 Rostock, Germany

[c]Faculty of Mechanical Engineering, Institute of Chemistry and Environmental Engineering, University of the Bundeswehr Munich, 85577 Neubiberg, Germany

[d]Photonion GmbH, 19061 Schwerin, Germany

[e]Chair of Piston Machines and Internal Combustion Engines, University of Rostock, 18059 Rostock, Germany

† Electronic supplementary information (ESI) available: Fig. S1: sum mass spectra without normalization. Fig. S2: sum mass spectra for 25% engine load. See DOI: https://doi.org/10.1039/d4ea00035h

‡ Currently at: Atmospheric Chemistry, Leibniz Institute for Tropospheric Research, Leipzig, Germany

© 2024 The Author(s). Published by the Royal Society of Chemistry

Open Access Article. Published on 20 May 2024. Downloaded on 11/15/2025 2:34:17 AM. This article is licensed under a Creative Commons Attribution 3.0 Unported Licence.

Ships are powered by large diesel engines that do not have the aftertreatment of exhaust gases that is common in road vehicles. Ship emissions aerosols are therefore part of diesel exhaust particles (DEP), which are classified by the International Agency for Research on Cancer (IARC) as a group 1 carcinogen with an increased risk of lung cancer. The particles (*e.g.* soot) also carry carcinogenic PAHs,[15–17] can cause oxidative stress and are cytotoxic.[18]

Even high-sulfur containing fuels can be legally used on ships if exhaust gas cleaning systems such as scrubbers reduce the sulfur emissions to levels similar to those of compliant fuels.[19] While ship emissions from fuels that comply with current regulations are reported to be reduced,[20–22] the use of wet scrubbers can still have a devastating impact on the environment.[23,24] One possible way to reduce both greenhouse gas and PM emissions from shipping is to use alternative fuels such as hydrotreated vegetable oil (HVO).[25] However, such fuels are costly and available only in limited quantities.[26,27]

The increased diversity of fuel types and the growing use of distillate fuels pose new challenges for air pollution monitoring, surveillance and source apportionment. The traditional markers of ship emissions are the transition metals V, Ni or Fe – *i.e.* residues from bunker fuels.[28] Based on these metals, single-particle mass spectrometry (SPMS) is capable to detect ship emissions in real time,[29–34] including complex atmospheric environments[33] even if scrubbers are used in SECAs.[31] However, the metals are not emitted during operation on distillate fuels and therefore new markers beyond the transition metals are needed.[28]

Characteristic patterns of volatile and semi-volatile aromatic hydrocarbons from ship emissions have been reported.[35] Recently, it was shown that ship emission particles from MGO combustion can be identified by their profile of PAHs,[36] using a new technology in single-particle mass spectrometry (SPMS).[37] Anders *et al.*[36] studied emissions from a research ship engine running on MGO and described a consistent PAH pattern with high homogeneity that was also found in marine ambient air. A transient appearance of this pattern could also be attributed to a distant ship passage, emphasizing the potential of single-particle PAH profiling as a novel marker concept for ship emissions from distillate fuels. The novel capability to characterize PAHs along with the inorganic composition of individual particles has sparked new applications and source apportionment capabilities.[38] Here we extend the new approach to currently relevant marine fuels and describe the single-particle PAH emissions from a research ship engine running on two HFOs with different sulfur contents, MGO and HVO. Complementary to the particle's inorganic composition, the PAH patterns we observed for our multi-fuel research engine provide the basis for a sophisticated approach to ship emission monitoring and control, covering and discriminating between different compliant and non-compliant fuels in real-time scenarios.[36,38]

Methods

Research ship engine, fuels and sampling

The experiments were carried out on a 1-cylinder, 4-stroke, 80 kW research marine engine with common rail injection, installed at the "Institute of Piston Machines and Internal Combustion Engines" in Rostock, Germany. This engine is a well-characterized model for ship emission studies and is suitable for all types of marine fuels.[39] The investigated fuels include (I) the SECA-compliant fuels MGO and HVO, (II) HFO with 0.5% FSC as a compliant fuel for waters outside SECAs, and (III) HFO with 2.4% FSC, which can only be used legally with sulfur scrubber technology. Further details on the fuel can be found elsewhere.[40] In addition, to show an appropriate range of engine operations, four different loads of 80 kW, 60 kW, 40 kW and 20 kW were investigated, corresponding to the relative engine loads of 100%, 75%, 50%, and 25%, respectively. All levels were operated for at least one hour, with a running-in period of 25 minutes for stabilization. The emitted aerosol was sampled and passed at a temperature of 200 °C through a cyclone with a cut-off size of 10 μm. The aerosol was diluted with dried and particle-free air in a two-stage ejector dilution system (eDiluter, Dekati Ltd, Finland). The dilution ratio was 1 : 50 for the experiments with the heavy fuel oils, while a dilution ratio of 1 : 25 was used for the MGO and HVO fuels, respectively. Finally, from a total flow of 1 L min^{-1} that was transported to the SPMS, 0.1 L min^{-1} was directed into the system. In addition to the SPMS' optical sizing unit, particle size distributions were also measured using a scanning mobility particle sizer (TSI; model 3082) downstream of the SPMS after further dilution by a factor of 100. Further detailed information on the sampling setup can be found in Jeong *et al.*[40]

Single-particle mass spectrometer with PAH characterization

The ability to measure chemical profiles of individual particles makes single-particle mass spectrometry (SPMS) a unique tool for source identification in complex atmospheric environments. Here, a novel ionization setup was applied, using spatially and temporally tailored laser pulses to simultaneously induce laser desorption/ionization (LDI) and resonance-enhanced multi-photon ionization (REMPI) of particle components. The technique provides single-particle information on the inorganic composition (*via* LDI) and particle-bound PAHs (*via* REMPI).[37] In brief, a narrow particle beam is formed by an aerodynamic lens at the inlet of the instrument. Individual particles in the beam are then optically detected and sized. Subsequently, each particle is exposed to an IR pulse from a CO_2 laser (10.6 μm, 20 mJ pulse energy), which desorbs organic matter and creates a gaseous plume surrounding the refractory particle residue. In the ionization step, an unfocused UV pulse from a KrF excimer laser (248 nm wavelength, 6 mJ pulse energy) ionizes the desorbed PAHs in the plume *via* REMPI.[41] The laser light is then backreflected and focused into the ion source, ionizing the refractory residue of the same particle *via* LDI at much higher laser intensity. PAH ions are measured in the positive arm of the bipolar Time-Of-Flight (TOF) mass spectrometer, while inorganic compounds from LDI are detected in both the positive and negative flight tubes. All ion signals are recorded by a 14 bit digitizer (ADQ14, Teledyne SP Devices AB, Sweden) and a customized software based on LabVIEW (National Instruments Inc.). It should be noted that SPMS data does not produce precise mass concentration values of the substances but yields

Open Access Article. Published on 20 May 2024. Downloaded on 11/15/2025 2:34:17 AM.
This article is licensed under a Creative Commons Attribution 3.0 Unported Licence.

chemical information on a single-particle level. Isobaric substances, however, cannot be distinguished (*e.g.* phenanthrene *vs.* anthracene).

Analysis of SPMS data

Custom MATLAB software (MathWorks Inc.) was used for the conversion of time-of-flight data to mass spectra with nominal mass resolution. The bars reflect the integrated peak area. Because of the different ionization processes, data from LDI and REMPI were individually normalized. The violin plots were created using the "violin plot" tool for matlab.[42] The principal component analysis (PCA) was performed on the time-of-flight data using the Matlab statistics toolbox with the "pca" command. Therefore, only PAH relevant data from REMPI were considered.

Results and discussion

Mass spectrometric pattern from different ship fuels

Fig. 1 shows the sum mass spectra of particles from engine operation with the different fuels during 60 kW (80%) load. The particle composition derived from LDI (black) reveals carbon clusters from soot as the dominant component of diesel exhaust particles (DEP), organic fragments and signals from lube oil constituents, *i.e.* calcium and phosphate.[43–46] The heavy fuel oils (Fig. 1(c) and (d)) produce the typical marker metals vanadium, iron and nickel. However, they appear relatively low due to the very strong Na^+ signal that dominates the normalized spectrum. The MGO and HVO emissions also reveal signals from these metals, however, with much lower peak intensities. They can originate from carry-over effects, *e.g. via* lube oil, and from redispersed particles from the inner surfaces of the manifold and exhaust.[44,45] Note that iron is resonantly ionized in our instrument, leading to substantial signal enhancements of the Fe^+ signal,[37,47] but also increased Ni^+ and V^+ peaks.[31] Due to their high sulfur content, heavy fuel oils show stronger sulfate signals compared to MGO and HVO. The difference for $^{97}HSO_4^-$ between the HFO fuels is only moderate due to signal saturation in the SPMS but it is noticeable for $^{80}SO_3^-$. Compared to MGO and HVO, the stronger alkali metal signals (Na^+ and K^+) are also noteworthy. For MGO, the inorganic particle composition from LDI resembles the results from previous studies on heavy-duty vehicles without exhaust filters.[45] For the heavy fuel oils, similar compositions have been reported in laboratory-based and field studies on ship emissions.[29–31,48,49]

The corresponding average PAH mass spectra from REMPI are shown in red in Fig. 1. For all fuels except HVO, these PAH signatures are dominated by series in m/z sequences of 14 Da starting at $m/z = 178$. The peak at $m/z = 178$ more likely stems from phenanthrene than from anthracene because the latter is predominantly formed in the combustion process[50] and associated with fewer alkylated derivatives, whereas alkylated phenanthrenes in the emissions are typical residues of unburned fuel.[35,36,39,51] For MGO, $m/z = 178$ is the dominant peak and the signals decrease with increasing degree of alkylation. This pattern has been described in detail in our previous study.[36] About 50% of the characterized particles from MGO combustion reveal clear PAH signals in their REMPI spectra.

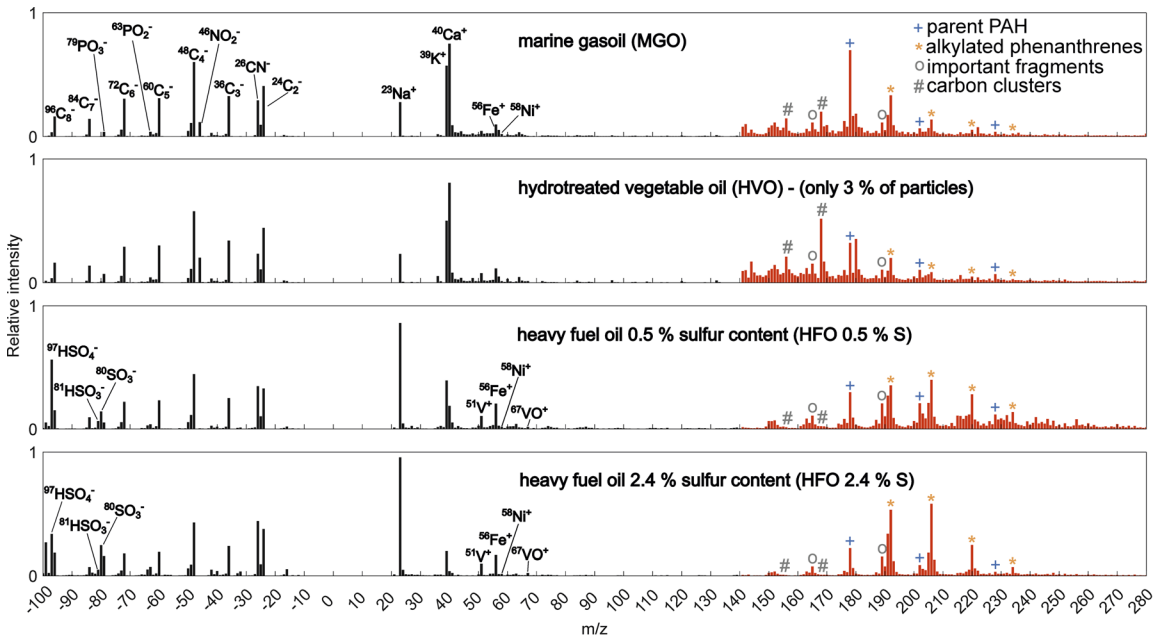

Fig. 1 Sum mass spectra ($n = 10\,000$) from laser desorption/ionization (LDI, black) and resonance-enhanced multiphoton ionization (REMPI, red) of particles from four marine fuels (75% engine load). The inorganic particle composition from the residual fuels exhibits the well-known signals of transition metals and sulfur. The PAH signals from MGO and HVO combustion show comparable pattern, while the total PAH signals for HVO are much smaller (balanced by normalization in the figure, see Fig. S1† for a comparison without normalization). For the HFO fuels, PAHs of higher mass are more pronounced and a higher degree of alkylation is observed, resulting in a shift of the maximum towards the C_2-phenanthrenes. The respective mass spectra for 25% engine load are shown in Fig. S2†.

 © 2024 The Author(s). Published by the Royal Society of Chemistry

Open Access Article. Published on 20 May 2024. Downloaded on 11/15/2025 2:34:17 AM.
This article is licensed under a Creative Commons Attribution 3.0 Unported Licence.

This value is comparable to the method's hit rate for PAHs[37] indicating that most particles contain PAHs, which is reasonable due to uniform condensation of semi-volatile organics on the particles in the exhaust. For the HVO combustion, the signal strength of PAHs and the fraction of PAH-containing particles is much smaller, with only 3% of particles showing a PAH signal well above the noise level. The signature of this small fraction of particles is comparable to that of the MGO particles (Fig. 1(b)), indicating that these signals result probably from resuspended particles from the exhaust rather than from the HVO combustion or fuel residues. This assumption is supported by fuel sample analyses, where PAHs in HVO were below the limits of detection, see Fig. S3.† Due to the HVO particle's low PAH content, high-mass carbon clusters are more pronounced in the normalized mass spectrum in Fig. 1(b). Similar to the MGO emissions, the particles from HFO combustion are characterized by a dominant series of alkylated phenanthrenes, however, the series extends to larger masses and its maximum is shifted to the C_2-phenanthrenes, resulting in a remarkably different pattern. There are also variations among the HFO fuels, *i.e.* stronger contributions from parent PAHs and high mass species for the low-sulfur HFO. However, compared to MGO, both HFO fuels share the distinct shift of the maximum towards the C_2-phenanthrenes.

The homogeneity of PAH signatures over the particle ensemble

For their use as a marker, it is crucial for the PAH signature to be stable across all emitted particles from one fuel. Although the inorganic composition of individual particles in engine emissions can vary significantly,[44,45] PAHs in ship emission particles from MGO combustion have already shown a higher degree of similarity.[36] Fig. 2 illustrates the distribution of congruence coefficients (r_c) as a measure of the similarity between the individual mass spectra. For each fuel, the congruence coefficient has been calculated for 5000 particles according to

$$r_c = \frac{\sum_{i,j} x_{i,j}^2 y_{i,j}^2}{\sqrt{\left(\sum_{i,j} x_{i,j}^2\right)\left(\sum_{i,j} y_{i,j}^2\right)}}$$

with x and y representing the single particle mass spectra. The median r_c value from REMPI signals represents the PAHs and is higher than the r_c from LDI signals that reveal the particle's inorganic composition, as evident from the violin plots in Fig. 2. For a direct comparison between the r_c values of all LDI and REMPI data at different engine loadings see Fig. S5 and S6.† Furthermore, the distribution of REMPI signals is notably denser for all fuels when compared to the signals in the LDI spectra and the interquartile range is small, demonstrating a high level of similarity for the PAH signatures. This supports the marker characteristics of PAHs in particle emissions from marine fuels.

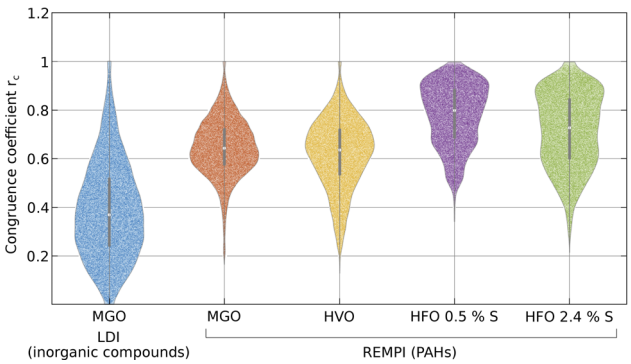

Fig. 2 Distribution of the congruence coefficients r_c between single-particle mass spectra of four different shipping fuels. The violin plot of r_c from the inorganic particle composition (LDI) of MGO particles reflects the heterogeneity of different particle types. In contrast, the REMPI signatures (mainly from PAHs) of the same particles from MGO combustion are more homogeneous. Also, for HVO, HFO with 0.5% sulfur, and HFO with 2.4% sulfur, the respective PAH patterns show a high homogeneity, which is a prerequisite for their use as a ship fuel marker. The width illustrates the number of particles in a bin. The interquartile range ($n = 5000$) that represents half of the particles is shown as a grey bar with its median in white.

Effect of the particle size

In addition to information on the particle composition, SPMS provides the individual particle size in vacuum aerodynamic diameter. The overall detection efficiency of the SPMS decreases rapidly for particles smaller than 200 nm, mainly due to the Mie scattering limit, which is strongly dependent on the wavelength of the continuous wave lasers in the optical sizing system.[52] To address this inherent bias of SPMS towards the largest size modes of combustion particles, we conducted additional measurements in the so-called 'free-running mode'. Ultrafine particles can be measured using this mode, which deactivates the optical detection and sizing unit while increasing the repetition rate of the desorption-and ionization lasers to 100 Hz in our experiment. The size limit for measured particles is reduced to approximately 50 nm at the expense of lost size information.[53,54] Fig. 3 illustrates the particle composition for different particle sizes. The averaged mass spectra of each 5000 particles are compared for both the free-running mode (including ultrafine particles, blue shaded) and the standard sizing mode ($\gtrsim$150 nm, red shaded). The respective particle size distributions were measured with a scanning mobility particle sizer (SMPS). For MGO and HVO, the measurements in free-running mode include the maximum of the size distribution and soot signatures are slightly increased relative to the larger particles measured in the sizing mode. Mass spectra obtained in the sizing mode show a phosphate signal that is 2 to 4 times more intense, an indication of a larger contribution from the lube oil. The particle size distributions of the heavy fuel oils are dominated by sulfate and soot particles,[55] which are too small to produce mass spectra in the instrument. Therefore, carbon clusters are not enhanced in the free-running mode. Consistent with our previous study,[36] the PAH patterns are not substantially affected by the particle size and retain their fuel-dependent signatures due to the uniform condensation of PAHs on the particles during cooling in the exhaust pipe. The size distribution data for each fuel under different load conditions can be found in the ESI in Fig. S4.†

Open Access Article. Published on 20 May 2024. Downloaded on 11/15/2025 2:34:17 AM.
This article is licensed under a Creative Commons Attribution 3.0 Unported Licence.

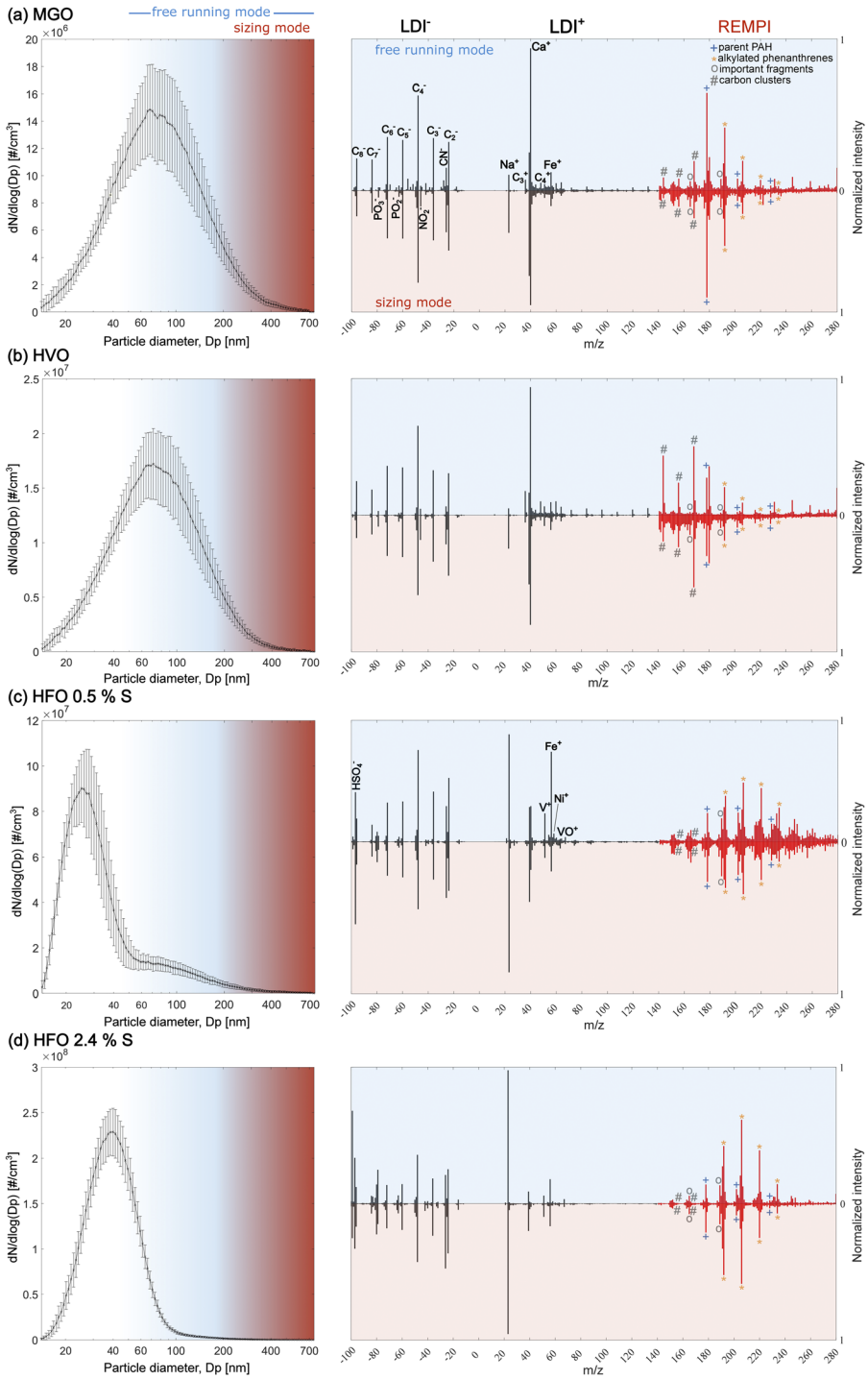

Fig. 3 (Left) Size distributions of (a) MGO, (b) HVO, (c) HFO 0.5% S, (d) HFO 2.4% S, measured using the scanning mobility particle sizer. The particle detection range of the single-particle mass spectrometer in free running mode is indicated by the blue shaded area. In this mode, particles of all sizes are hit at random and size information is not available. The red area indicates the coverage in normal sizing mode. The right side shows the normalized sum spectra of each 5000 particles, respectively, in both the free-running mode (blue shaded) and sizing mode (red shaded). The free-running mode includes smaller particles and reveals more pronounced contributions from soot (see MGO and HVO) while the sizing mode covers only large particles (≳150 nm) and exhibits 2–4 times stronger phosphate signals from lube oil. The PAH mass spectra are hardly affected by the particle size and reveal their distinct patterns for each individual fuel.

Fuel-specific characteristics of PAH signatures

To investigate a measure of fuel differentiation and the influence of load conditions, a principal component analysis (PCA) was performed on the PAH mass spectra of the particles from all fuels at two different engine loads. As an exploratory analysis, the first two principal components were considered, covering

 © 2024 The Author(s). Published by the Royal Society of Chemistry

Open Access Article. Published on 20 May 2024. Downloaded on 11/15/2025 2:34:17 AM.
This article is licensed under a Creative Commons Attribution 3.0 Unported Licence.

57% of the total variance. The biplot (Fig. 4) illustrates the relation between the factors "fuel" and "load" from PC scores and provide information on the variables responsible for grouping from the PC loadings. A separation along the first PC into HFO and the fuels MGO and HVO can be noticed. HFO contains longer alkylated alkyl chains in the homologue series of phenanthrene, which is the driver of the fuel separation because unburned fuel is the main contributor to aromatic compounds in particulate emissions. Peaks of C_2- to-C_4-alkylated phenanthrenes appear at $m/z = 206$, 220 and 234, while the peak at $m/z = 189$ denotes a common fragment of angled PAH with larger degrees of alkylation.[56,57] Except for MGO and HVO, the variances within the two fuel types, highlighted by the 95% confident ellipses, were apparently lower than between them, thus supporting the use of this signature for ship fuel identification. Note that the HVO in this study only serves as the "cleanest" possible hydrocarbon fuel. Engine operation at lower loads causes emissions with a higher contribution of unburned fuel than higher loads. In the PCA biplot, the effect of engine load appears in the vertical direction on the second PC for all fuels, although minor in the case of HVO. Emissions at higher engine loads contain more aromatics from high-temperature pyrosynthesis inside the combustion chamber, such as by the hydrogen-abstraction carbon-addition (HACA) mechanism.[58] Variables pulling in the positive direction of PC2 are $m/z = 178$ and $m/z = 192$, *i.e.* phenanthrenes of no or low degree of alkylation, indicating pyrosynthesis and a lower contribution of unburned fuel. Conversely, alkylated phenanthrenes at $m/z =$ 206, 220 and 234 show contributions in the negative direction of PC2, thus towards low engine loads. Nevertheless, variances added by the actor "load" are lower than for the factor "fuel", hence the fuel type has a stronger effect on the mass spectral signatures in the particle ensemble, emphasizing the identification of the used ship fuel by our SPMS approach.

Potential and limitations for the PAHs as fuel markers in SPMS

Our study shows that many of the conditions are in place for the use of single-particle PAH signatures as a future marine fuel marker. In particular, the characteristic PAH pattern unique to the fuel is evident for most particles and is consistent with particle size and engine load. The HVO emissions are difficult to identify due to the low number of particles with PAHs and the similarity to the MGO pattern, but the relevance of HVO for the future shipping industry is questionable.[59,60] The inorganic particle composition remains detectable with our SPMS-method. In a screening approach it can further help to distinguish between *e.g.* high sulfur and low sulfur blends or between metal-containing residual fuels and distillates, which are often named "hybrid" fuels. Higher confidence in identification may be achieved with our complementary PAH analysis. One aspect that is difficult to investigate is the effect of engine type and engine size. However, as fuel residues are a major determinant of the PAH signal, the inevitable emission of unburnt fuel will contribute to signal consistency between different ships. In a previous study, we discussed potential interferences between MGO combustion and terrestrial emissions and concluded that,

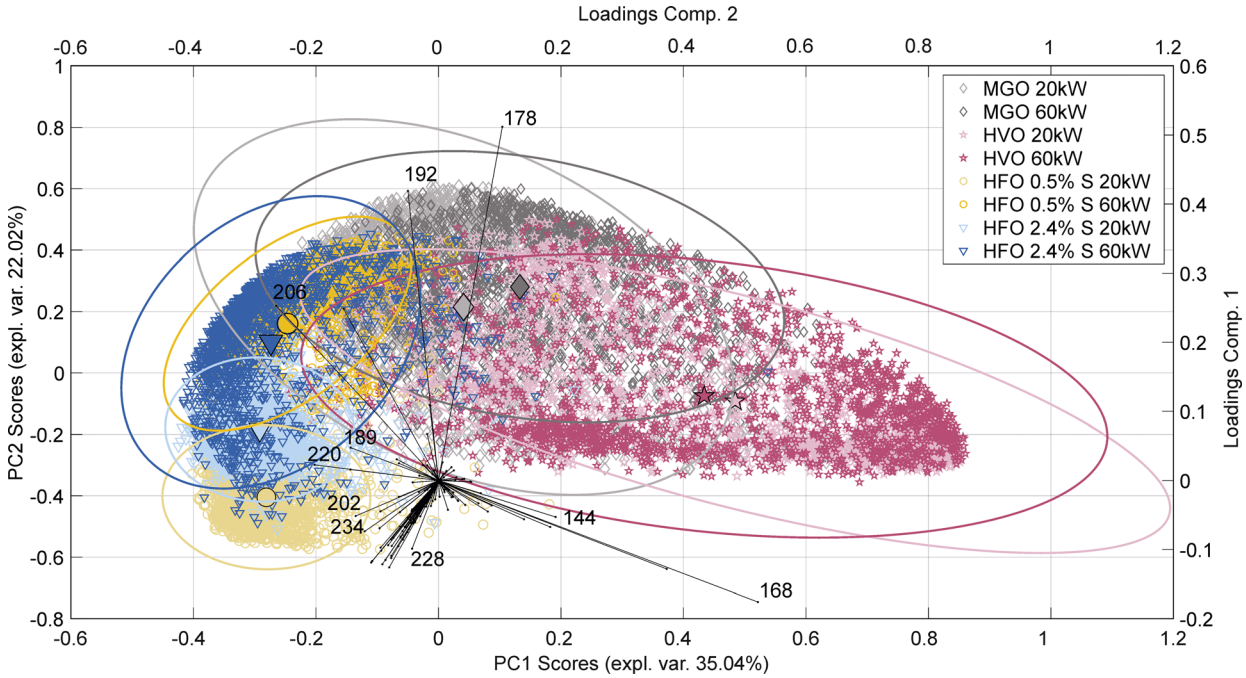

Fig. 4 Principal component analysis of single-particle PAH mass spectra from marine gasoil (grey), hydrotreated vegetable oil (red), heavy fuel oil 0.5% sulfur (blue) and heavy fuel oil 2.4% sulfur (yellow) at 20 kW load and 60 kW load, respectively. The length of the eigenvectors represents the contribution of signals at different mass-to-charge ratios to the mass spectral differences. The ellipses depict the 95% confidence interval for the principal component scores of each cluster. While the clusters are well separated for the low load conditions (light colors), the mass spectral signatures approach each other at higher load (dark colors), but remain distinguishable. $N = 1670$ for each of the fuels and loads.

Open Access Article. Published on 20 May 2024. Downloaded on 11/15/2025 2:34:17 AM. This article is licensed under a Creative Commons Attribution 3.0 Unported Licence.

due to the widespread use of filter technologies, only a few land-based sources with comparable PAH emission patterns remain, namely diesel engines without exhaust filters, *e.g.* at power generators, construction machines, and old vehicles.[36] The same interferences can also be expected for the HFO emissions with their alkylated PAHs of higher masses. An important terrestrial PAH source is wood combustion. In comparison to ship emission particles, SPMS mass spectra from wood combustion show much stronger parent PAH signals (see *e.g.* ESI† in Anders *et al.* 2023 (ref. 36)). The series of alkylated phenanthrenes in the PAH spectra from HFO shows some similarities to emissions from the smouldering combustion of biomass material.[61] However, while the decomposition of resin acids in wood burning typically results in a (local) maximum of the phenanthrenes at $m/z = 234$,[62,63] the HFO produces a smooth distribution with its maximum at lower masses, see Fig. 1. Nevertheless, with the additional information about the particle's inorganic composition, a straightforward differentiation between the fossil residual fuel (strong sulfur and metal signals) and the biomass fuel (dominant potassium signal[64–66]) is possible. In a field study of PAHs in aerosols using the same method at the Swedish coast, we found no PAH signatures similar to the HFO pattern in >290 000 particles, of which >4000 had detailed PAH mass spectra.[38] Given the large distance to the SECA outer boundary (>1000 km) and the high fuel compliance within the Baltic SECA,[67] this may not be surprising, but it also indicates the absence of other sources with a similar PAH signature.

Another source of ambiguity is related to the degradation of PAHs. Substance-specific rates introduce an important limitation to the diagnostic ratio concept in source apportionment.[68,69] The degradation of PAHs may not be an important factor in the detection and monitoring of individual ship plumes, as the plumes disintegrate within minutes to a few hours.[70] For assessments of the contribution of shipping to background air pollution and for studies of long-range transport, PAH degradation may be a major limitation of the approach. However, PAHs have often been shown to persist in the atmosphere for much longer than suggested by laboratory experiments,[69] *e.g.* because of weather conditions and slower dark ageing[71] or due to shielding effects.[72,73]

Conclusion and outlook

Having introduced the concept of single-particle PAH pattern as a marker for ship emissions from distillate fuel combustion,[36] here we extend this approach to other relevant ship fuels. As unburnt fuel residues contribute significantly to the PAH signatures, the patterns retain their fuel-characteristic profiles under different conditions and are also expected to have a high degree of similarity between different marine engines. The basic field-applicability of the PAH marker approach could already be shown,[36] however, field studies should demonstrate the differentiability of the various fuels for a larger number of ship plumes. This is a challenging task due to fuel uniformity and high compliance rates in SECAs,[67] and it may require open-sea measurements outside the SECA to get data from a sufficient number of ships with different fuels.[74] However, previous research and this study demonstrate the potential of PAHs as fuel markers for ships in the area of source apportionment, where it is difficult to find a long-range method to ensure compliance in emission control areas.

Author contributions

L. A., J. S. and I.-E. R. performed the SPMS experiments. L. A. and H. C. analyzed the data. R. I. provided technical assistance. U. K. and T. G. analyzed the fuel samples. U. E., S. J., M. R. S. B. and J. B. performed the aerosol characterization experiments at the engine. U. E. and B. B. provided the research ship engine and operated it. T. S., B. B. and R. Z. developed and managed the project and raised funding. J. S., M. S., H. C., T. A. and R. Z. gave scientific discussions. J. P. conceived the study. L. A. and J. P. wrote the manuscript.

Conflicts of interest

There are no conflicts to declare.

Acknowledgements

This research has been supported by the German Federal Ministry for Economic Affairs and Climate Action (SAARUS project, grant no. 03SX483D), and by the Helmholtz Association (International Laboratory aeroHEALTH – Interlabs-0005). Funded by the Deutsche Forschungsgemeinschaft (DFG, German Research Foundation) – SFB 1477 "Light–Matter Interactions at Interfaces", project number 441234705.

References

1 J. Fuglestvedt, T. Berntsen, V. Eyring, I. Isaksen, D. S. Lee and R. Sausen, Shipping emissions: from cooling to warming of climate-and reducing impacts on health, *Environ. Sci. Technol.*, 2009, **43**, 9057–9062.
2 E. Ytreberg, S. Åström and E. Fridell, Valuating environmental impacts from ship emissions – The marine perspective, *J. Environ. Manage.*, 2021, **282**, 111958.
3 J. J. Corbett, J. J. Winebrake, E. H. Green, P. Kasibhatla, V. Eyring and A. Lauer, Mortality from ship emissions: a global assessment, *Environ. Sci. Technol.*, 2007, **41**, 8512–8518.
4 V. Eyring, J. J. Corbett, D. S. Lee and J. J. Winebrake, Brief summary of the impact of ship emissions on atmospheric composition, climate, and human health, 2024, **http://www.pa.op.dlr.de/~VeronikaEyring/Eyringetal_IMOBriefSummary_FINAL.pdf**, accessed 7 May.
5 N. Mueller, M. Westerby and M. Nieuwenhuijsen, Health impact assessments of shipping and port-sourced air pollution on a global scale: A scoping literature review, *Environ. Res.*, 2023, **216**, 114460.
6 C. Geels, M. Winther, C. Andersson, J.-P. Jalkanen, J. Brandt, L. M. Frohn, U. Im, W. Leung and J. H. Christensen, Projections of shipping emissions and the related impact

 © 2024 The Author(s). Published by the Royal Society of Chemistry

Open Access Article. Published on 20 May 2024. Downloaded on 11/15/2025 2:34:17 AM.
This article is licensed under a Creative Commons Attribution 3.0 Unported Licence.

on air pollution and human health in the Nordic region, *Atmos. Chem. Phys.*, 2021, **21**, 12495–12519.

7 Facts about maritime shipping and its environmental impact, 2024, https://www.umweltbundesamt.de/en/topics/water/seas/maritime-shipping#facts-about-maritime-shipping-and-its-environmental-impact, accessed 9 February.

8 E. Commission, CE_Delft_7M92_Study_on_methods_and_considerations_for_the_determination_of_greenhouse_gas_Def, 2024, https://cedelft.eu/wp-content/uploads/sites/2/2021/03/CE_Delft_7M92_Study_on_methods_and_considerations_for_the_determination_of_greenhouse_gas_Def.pdf, accessed 9 February.

9 Ships face lower sulphur fuel requirements in emission control areas from 1 January 2015, 2024, https://www.imo.org/en/MediaCentre/PressBriefings/Pages/44-ECA-sulphur.aspx, accessed 9 February.

10 J. E. Jonson, M. Gauss, M. Schulz, J.-P. Jalkanen and H. Fagerli, Effects of global ship emissions on European air pollution levels, *Atmos. Chem. Phys.*, 2020, **20**, 11399–11422.

11 J. Antturi, O. Hänninen, J.-P. Jalkanen, L. Johansson, M. Prank, M. Sofiev and M. Ollikainen, Costs and benefits of low-sulphur fuel standard for Baltic Sea shipping, *J. Environ. Manage.*, 2016, **184**, 431–440.

12 T. Chu Van, J. Ramirez, T. Rainey, Z. Ristovski and R. J. Brown, Global impacts of recent IMO regulations on marine fuel oil refining processes and ship emissions, *Transp. Res. D: Transp. Environ.*, 2019, **70**, 123–134.

13 S. D. Seppälä, J. Kuula, A.-P. Hyvärinen, S. Saarikoski, T. Rönkkö, J. Keskinen, J.-P. Jalkanen and H. Timonen, Effects of marine fuel sulfur restrictions on particle number concentrations and size distributions in ship plumes in the Baltic Sea, *Atmos. Chem. Phys.*, 2021, **21**, 3215–3234.

14 S. Oeder, T. Kanashova, O. Sippula, S. C. Sapcariu, T. Streibel, J. M. Arteaga-Salas, J. Passig, M. Dilger, H.-R. Paur, C. Schlager, S. Mülhopt, S. Diabaté, C. Weiss, B. Stengel, R. Rabe, H. Harndorf, T. Torvela, J. K. Jokiniemi, M.-R. Hirvonen, C. Schmidt-Weber, C. Traidl-Hoffmann, K. A. BéruBé, A. J. Wlodarczyk, Z. Prytherch, B. Michalke, T. Krebs, A. S. H. Prévôt, M. Kelbg, J. Tiggesbäumker, E. Karg, G. Jakobi, S. Scholtes, J. Schnelle-Kreis, J. Lintelmann, G. Matuschek, M. Sklorz, S. Klingbeil, J. Orasche, P. Richthammer, L. Müller, M. Elsasser, A. Reda, T. Gröger, B. Weggler, T. Schwemer, H. Czech, C. P. Rüger, G. Abbaszade, C. Radischat, K. Hiller, J. T. M. Buters, G. Dittmar and R. Zimmermann, Particulate matter from both heavy fuel oil and diesel fuel shipping emissions show strong biological effects on human lung cells at realistic and comparable in vitro exposure conditions, *PLoS One*, 2015, **10**, e0126536.

15 N. Rajput and A. Lakhani, PAHs and their Carcinogenic Potencies in Diesel Fuel and Diesel Generator Exhaust, *Hum. Ecol. Risk Assess.*, 2009, **15**, 201–213.

16 S. Zhou, J. Zhou and Y. Zhu, Chemical composition and size distribution of particulate matters from marine diesel engines with different fuel oils, *Fuel*, 2019, **235**, 972–983.

17 L. Benbrahim-Tallaa, R. A. Baan, Y. Grosse, B. Lauby-Secretan, F. El Ghissassi, V. Bouvard, N. Guha, D. Loomis and K. Straif, Carcinogenicity of diesel-engine and gasoline-engine exhausts and some nitroarenes, *Lancet Oncol.*, 2012, **13**, 663–664.

18 D. Wu, Q. Li, X. Ding, J. Sun, D. Li, H. Fu, M. Teich, X. Ye and J. Chen, Primary Particulate Matter Emitted from Heavy Fuel and Diesel Oil Combustion in a Typical Container Ship: Characteristics and Toxicity, *Environ. Sci. Technol.*, 2018, **52**, 12943–12951.

19 L. Osipova, E. Georgeff and B. Comer, Global scrubber washwater discharges under IMO's 2020 fuel sulfur limit, 2024, https://theicct.org/wp-content/uploads/2021/06/scrubber-discharges-Apr2021.pdf, accessed 9 January.

20 J. E. Jonson, M. Gauss, J.-P. Jalkanen and L. Johansson, Effects of strengthening the Baltic Sea ECA regulations, *Atmos. Chem. Phys.*, 2019, **19**, 13469–13487.

21 M. Viana, V. Rizza, A. Tobías, E. Carr, J. Corbett, M. Sofiev, A. Karanasiou, G. Buonanno and N. Fann, Estimated health impacts from maritime transport in the Mediterranean region and benefits from the use of cleaner fuels, *Environ. Int.*, 2020, **138**, 105670.

22 V. Zisi, H. N. Psaraftis and T. Zis, The impact of the 2020 global sulfur cap on maritime CO2 emissions, *Marit. Bus. Rev.*, 2021, **6**, 339–357.

23 A. Lunde Hermansson, I.-M. Hassellöv, J. Moldanová and E. Ytreberg, Comparing emissions of polyaromatic hydrocarbons and metals from marine fuels and scrubbers, *Transp. Res. D: Transp. Environ.*, 2021, **97**, 102912.

24 H. Winnes, E. Fridell and J. Moldanová, Effects of Marine Exhaust Gas Scrubbers on Gas and Particle Emissions, *J. Manuf. Sci. Eng.*, 2020, **8**, 299.

25 S. Ushakov and N. Lefebvre, Assessment of Hydrotreated Vegetable Oil (HVO) Applicability as an Alternative Marine Fuel Based on Its Performance and Emissions Characteristics, *SAE Int. J. Fuels Lubr.*, 2019, **12**(2), 109–120.

26 T. Solakivi, A. Paimander and L. Ojala, Cost competitiveness of alternative maritime fuels in the new regulatory framework, *Transp. Res. D: Transp. Environ.*, 2022, **113**, 103500.

27 Rotterdam Bunker Prices, 2024, https://shipandbunker.com/prices/emea/nwe/nl-rtm-rotterdam#ULSFO, accessed 9 February.

28 H. Czech, J. Schnelle-Kreis, T. Streibel and R. Zimmermann, New directions: Beyond sulphur, vanadium and nickel – About source apportionment of ship emissions in emission control areas, *Atmos. Environ.*, 2017, **163**, 190–191.

29 R. M. Healy, I. P. O'Connor, S. Hellebust, A. Allanic, J. R. Sodeau and J. C. Wenger, Characterisation of single particles from in-port ship emissions, *Atmos. Environ.*, 2009, **43**, 6408–6414.

30 A. P. Ault, C. I. Gaston, Y. Wang, G. Dominguez, M. H. Thiemens and K. A. Prather, Characterization of the single particle mixing state of individual ship plume events

Open Access Article. Published on 20 May 2024. Downloaded on 11/15/2025 2:34:17 AM.
This article is licensed under a Creative Commons Attribution 3.0 Unported Licence.

measured at the Port of Los Angeles, *Environ. Sci. Technol.*, 2010, **44**, 1954–1961.

31 J. Passig, J. Schade, R. Irsig, L. Li, X. Li, Z. Zhou, T. Adam and R. Zimmermann, Detection of ship plumes from residual fuel operation in emission control areas using single-particle mass spectrometry, *Atmos. Meas. Tech.*, 2021, **14**, 4171–4185.

32 J. Zhao, Y. Zhang, H. Xu, S. Tao, R. Wang, Q. Yu, Y. Chen, Z. Zou and W. Ma, Trace Elements From Ocean-Going Vessels in East Asia: Vanadium and Nickel Emissions and Their Impacts on Air Quality, *J. Geophys. Res.: Atmos.*, 2021, **126**(8), DOI: 10.1029/2020JD033984.

33 X. Xiong, Z. Wang, C. Cheng, M. Li, L. Yun, S. Liu, L. Mao and Z. Zhou, Long-Term Observation of Mixing States and Sources of Vanadium-Containing Single Particles from 2020 to 2021 in Guangzhou, China, *Toxics*, 2023, **11**(4), 339.

34 E. I. Rosewig, J. Schade, J. Passig, H. Osterholz, R. Irsig, D. Smok, N. Gawlitta, J. Schnelle-Kreis, J. Hovorka, D. Schulz-Bull, R. Zimmermann and T. W. Adam, Remote Detection of Different Marine Fuels in Exhaust Plumes by Onboard Measurements in the Baltic Sea Using Single-Particle Mass Spectrometry, *Atmosphere*, 2023, **14**, 849.

35 H. Czech, B. Stengel, T. Adam, M. Sklorz, T. Streibel and R. Zimmermann, A chemometric investigation of aromatic emission profiles from a marine engine in comparison with residential wood combustion and road traffic: Implications for source apportionment inside and outside sulphur emission control areas, *Atmos. Environ.*, 2017, **167**, 212–222.

36 L. Anders, J. Schade, E. I. Rosewig, T. Kröger-Badge, R. Irsig, S. Jeong, J. Bendl, M. R. Saraji-Bozorgzad, J.-H. Huang, F.-Y. Zhang, C. C. Wang, T. Adam, M. Sklorz, U. Etzien, B. Buchholz, H. Czech, T. Streibel, J. Passig and R. Zimmermann, Detection of ship emissions from distillate fuel operation via single-particle profiling of polycyclic aromatic hydrocarbons, *Environ. Sci.: Atmos.*, 2023, **3**, 1134–1144.

37 J. Schade, J. Passig, R. Irsig, S. Ehlert, M. Sklorz, T. Adam, C. Li, Y. Rudich and R. Zimmermann, Spatially Shaped Laser Pulses for the Simultaneous Detection of Polycyclic Aromatic Hydrocarbons as well as Positive and Negative Inorganic Ions in Single Particle Mass Spectrometry, *Anal. Chem.*, 2019, **91**, 10282–10288.

38 J. Passig, J. Schade, R. Irsig, T. Kröger-Badge, H. Czech, T. Adam, H. Fallgren, J. Moldanova, M. Sklorz, T. Streibel and R. Zimmermann, Single-particle characterization of polycyclic aromatic hydrocarbons in background air in northern Europe, *Atmos. Chem. Phys.*, 2022, **22**, 1495–1514.

39 T. Streibel, J. Schnelle-Kreis, H. Czech, H. Harndorf, G. Jakobi, J. Jokiniemi, E. Karg, J. Lintelmann, G. Matuschek, B. Michalke, L. Müller, J. Orasche, J. Passig, C. Radischat, R. Rabe, A. Reda, C. Rüger, T. Schwemer, O. Sippula, B. Stengel, M. Sklorz, T. Torvela, B. Weggler and R. Zimmermann, Aerosol emissions of a ship diesel engine operated with diesel fuel or heavy fuel oil, *Environ. Sci. Pollut. Res. Int.*, 2017, **24**, 10976–10991.

40 S. Jeong, J. Bendl, M. Saraji-Bozorgzad, U. Käfer, U. Etzien, J. Schade, M. Bauer, G. Jakobi, J. Orasche, K. Fisch, P. P. Cwierz, C. P. Rüger, H. Czech, E. Karg, G. Heyen, M. Krausnick, A. Geissler, C. Geipel, T. Streibel, J. Schnelle-Kreis, M. Sklorz, D. E. Schulz-Bull, B. Buchholz, T. Adam and R. Zimmermann, Aerosol emissions from a marine diesel engine running on different fuels and effects of exhaust gas cleaning measures, *Environ. Pollut.*, 2023, **316**, 120526.

41 C. Gehm, T. Streibel, J. Passig and R. Zimmermann, Determination of Relative Ionization Cross Sections for Resonance Enhanced Multiphoton Ionization of Polycyclic Aromatic Hydrocarbons, *Appl. Sci.*, 2018, **8**(9), 1617.

42 H. Hoffmann, *Violin Plot. MATLAB Central File Exchange*, 2024, https://de.mathworks.com/matlabcentral/fileexchange/45134-violin-plot, accessed 7 May.

43 D. A. Sodeman, S. M. Toner and K. A. Prather, Determination of single particle mass spectral signatures from light-duty vehicle emissions, *Environ. Sci. Technol.*, 2005, **39**, 4569–4580.

44 S. M. Toner, D. A. Sodeman and K. A. Prather, Single particle characterization of ultrafine and accumulation mode particles from heavy duty diesel vehicles using aerosol time-of-flight mass spectrometry, *Environ. Sci. Technol.*, 2006, **40**, 3912–3921.

45 L. G. Shields, D. T. Suess and K. A. Prather, Determination of single particle mass spectral signatures from heavy-duty diesel vehicle emissions for PM2.5 source apportionment, *Atmos. Environ.*, 2007, **41**, 3841–3852.

46 M. T. Spencer, L. G. Shields, D. A. Sodeman, S. M. Toner and K. A. Prather, Comparison of oil and fuel particle chemical signatures with particle emissions from heavy and light duty vehicles, *Atmos. Environ.*, 2006, **40**, 5224–5235.

47 J. Passig, J. Schade, E. I. Rosewig, R. Irsig, T. Kröger-Badge, H. Czech, M. Sklorz, T. Streibel, L. Li, X. Li, Z. Zhou, H. Fallgren, J. Moldanova and R. Zimmermann, Resonance-enhanced detection of metals in aerosols using single-particle mass spectrometry, *Atmos. Chem. Phys.*, 2020, **20**, 7139–7152.

48 Z. Liu, X. Lu, J. Feng, Q. Fan, Y. Zhang and X. Yang, Influence of Ship Emissions on Urban Air Quality: A Comprehensive Study Using Highly Time-Resolved Online Measurements and Numerical Simulation in Shanghai, *Environ. Sci. Technol.*, 2017, **51**, 202–211.

49 L. Zhou, M. Li, C. Cheng, Z. Zhou, H. Nian, R. Tang and C. K. Chan, Real-time chemical characterization of single ambient particles at a port city in Chinese domestic emission control area - Impacts of ship emissions on urban air quality, *Sci. Total Environ.*, 2022, **819**, 153117.

50 J. T. Andersson and C. Achten, Time to Say Goodbye to the 16 EPA PAHs? Toward an Up-to-Date Use of PACs for Environmental Purposes, *Polycycl. Aromat. Comp.*, 2015, **35**, 330–354.

51 C. Radischat, O. Sippula, B. Stengel, S. Klingbeil, M. Sklorz, R. Rabe, T. Streibel, H. Harndorf and R. Zimmermann, Real-time analysis of organic compounds in ship engine aerosol emissions using resonance-enhanced multiphoton ionisation and proton transfer mass spectrometry, *Anal. Bioanal. Chem.*, 2015, **407**, 5939–5951.

 © 2024 The Author(s). Published by the Royal Society of Chemistry

Open Access Article. Published on 20 May 2024. Downloaded on 11/15/2025 2:34:17 AM.
This article is licensed under a Creative Commons Attribution 3.0 Unported Licence.

52 G. S. He, H.-Y. Qin and Q. Zheng, Rayleigh, Mie, and Tyndall scatterings of polystyrene microspheres in water: Wavelength, size, and angle dependences, *J. Appl. Phys.*, 2009, **105**, 023110.
53 Y. Su, M. F. Sipin, H. Furutani and K. A. Prather, Development and characterization of an aerosol time-of-flight mass spectrometer with increased detection efficiency, *Anal. Chem.*, 2004, **76**, 712–719.
54 W. D. Reents and Z. Ge, Simultaneous Elemental Composition and Size Distributions of Submicron Particles in Real Time Using Laser Atomization/Ionization Mass Spectrometry, *Aerosol Sci. Technol.*, 2010, **33**, 122–134.
55 Q. Xiao, M. Li, H. Liu, M. Fu, F. Deng, Z. Lv, H. Man, X. Jin, S. Liu and K. He, Characteristics of marine shipping emissions at berth: profiles for particulate matter and volatile organic compounds, *Atmos. Chem. Phys.*, 2018, **18**, 9527–9545.
56 Y. Zhao, B. Hong, Y. Fan, M. Wen and X. Han, Accurate analysis of polycyclic aromatic hydrocarbons (PAHs) and alkylated PAHs homologs in crude oil for improving the gas chromatography/mass spectrometry performance, *Ecotoxicol. Environ. Saf.*, 2014, **100**, 242–250.
57 C. Kruth, H. Czech, M. Sklorz, J. Passig, S. Ehlert, A. Cappiello and R. Zimmermann, Direct Infusion Resonance-Enhanced Multiphoton Ionization Mass Spectrometry of Liquid Samples under Vacuum Conditions, *Anal. Chem.*, 2017, **89**, 10917–10923.
58 M. Frenklach, Reaction mechanism of soot formation in flames, *Phys. Chem. Chem. Phys.*, 2002, **4**, 2028–2037.
59 R. McGill, W. Remley and K. Winther, Alternative Fuels for Marine Applications, 2024, **https://www.methanol.org/wp-content/uploads/2016/07/AMF_Annex_41-Alt-Fuels-for-Marine-May-2013.pdf**, accessed 10 January.
60 M. Aarnio, *Cruise Ship Handbook*, Springer International Publishing; Imprint Springer, Cham, 1st edn, 2023.
61 C. Li, Q. He, J. Schade, J. Passig, R. Zimmermann, D. Meidan, A. Laskin and Y. Rudich, Dynamic changes in optical and chemical properties of tar ball aerosols by atmospheric photochemical aging, *Atmos. Chem. Phys.*, 2019, **19**, 139–163.
62 P. Martens, H. Czech, J. Orasche, G. Abbaszade, M. Sklorz, B. Michalke, J. Tissari, T. Bizjak, M. Ihalainen, H. Suhonen, P. Yli-Pirilä, J. Jokiniemi, O. Sippula and R. Zimmermann, Brown Coal and Logwood Combustion in a Modern Heating Appliance: The Impact of Combustion Quality and Fuel on Organic Aerosol Composition, *Environ. Sci. Technol.*, 2023, **57**, 5532–5543.
63 H. Czech, T. Miersch, J. Orasche, G. Abbaszade, O. Sippula, J. Tissari, B. Michalke, J. Schnelle-Kreis, T. Streibel, J. Jokiniemi and R. Zimmermann, Chemical composition and speciation of particulate organic matter from modern residential small-scale wood combustion appliances, *Sci. Total Environ.*, 2018, **612**, 636–648.
64 J. Arndt, J. Sciare, M. Mallet, G. C. Roberts, N. Marchand, K. Sartelet, K. Sellegri, F. Dulac, R. M. Healy and J. C. Wenger, Sources and mixing state of summertime background aerosol in the north-western Mediterranean basin, *Atmos. Chem. Phys.*, 2017, **17**, 6975–7001.
65 M. Dall'Osto, D. C. S. Beddows, E. J. McGillicuddy, J. K. Esser-Gietl, R. M. Harrison and J. C. Wenger, On the simultaneous deployment of two single-particle mass spectrometers at an urban background and a roadside site during SAPUSS, *Atmos. Chem. Phys.*, 2016, **16**, 9693–9710.
66 F. Köllner, J. Schneider, M. D. Willis, T. Klimach, F. Helleis, H. Bozem, D. Kunkel, P. Hoor, J. Burkart, W. R. Leaitch, A. A. Aliabadi, J. P. D. Abbatt, A. B. Herber and S. Borrmann, Particulate trimethylamine in the summertime Canadian high Arctic lower troposphere, *Atmos. Chem. Phys.*, 2017, **17**, 13747–13766.
67 A. Lähteenmäki-Uutela, J. Yliskylä-Peuralahti, S. Repka and J. Mellqvist, What explains SECA compliance: rational calculation or moral judgment?, *WMU J. Marit. Aff.*, 2019, **18**, 61–78.
68 M. Tobiszewski and J. Namieśnik, PAH diagnostic ratios for the identification of pollution emission sources, *Environ. Pollut.*, 2012, **162**, 110–119.
69 I. J. Keyte, R. M. Harrison and G. Lammel, Chemical reactivity and long-range transport potential of polycyclic aromatic hydrocarbons – a review, *Chem. Soc. Rev.*, 2013, **42**, 9333–9391.
70 A. Petzold, J. Hasselbach, P. Lauer, R. Baumann, K. Franke, C. Gurk, H. Schlager and E. Weingartner, Experimental studies on particle emissions from cruising ship, their characteristic properties, transformation and atmospheric lifetime in the marine boundary layer, *Atmos. Chem. Phys.*, 2008, **8**, 2387–2403.
71 U. Pöschl, T. Letzel, C. Schauer and R. Niessner, Interaction of Ozone and Water Vapor with Spark Discharge Soot Aerosol Particles Coated with Benzo[a]pyrene: O 3 and H 2 O Adsorption, Benzo[a]pyrene Degradation, and Atmospheric Implications, *J. Phys. Chem. A*, 2001, **105**, 4029–4041.
72 S. Zhou, A. K. Y. Lee, R. D. McWhinney and J. P. D. Abbatt, Burial effects of organic coatings on the heterogeneous reactivity of particle-borne benzoapyrene (BaP) toward ozone, *J. Phys. Chem. A*, 2012, **116**, 7050–7056.
73 M. Shrivastava, S. Lou, A. Zelenyuk, R. C. Easter, R. A. Corley, B. D. Thrall, P. J. Rasch, J. D. Fast, S. L. Massey Simonich, H. Shen and S. Tao, Global long-range transport and lung cancer risk from polycyclic aromatic hydrocarbons shielded by coatings of organic aerosol, *Proc. Natl. Acad. Sci. U. S. A.*, 2017, **114**, 1246–1251.
74 S. Celik, F. Drewnick, F. Fachinger, J. Brooks, E. Darbyshire, H. Coe, J.-D. Paris, P. G. Eger, J. Schuladen, I. Tadic, N. Friedrich, D. Dienhart, B. Hottmann, H. Fischer, J. N. Crowley, H. Harder and S. Borrmann, Influence of vessel characteristics and atmospheric processes on the gas and particle phase of ship emission plumes: in situ measurements in the Mediterranean Sea and around the Arabian Peninsula, *Atmos. Chem. Phys.*, 2020, **20**, 4713–4734.